

JET PROPULSION LABORATORY INTEROFFICE MEMORANDUM

AIRS ADF#1108

February 5, 2025

To: Distribution

From: T. Pagano (Jet Propulsion Laboratory, California Institute of Technology)

CC: S. Broberg, H. Aumann, E. Manning, R. Wilson, J. Teixeira, E. Fetzer, H. Thrastarson, K. Overoye, H. Revercomb (UW), D. Tobin (UW)

Subject: Ancillary data for AIRS OBC Blackbody

References:

1. Pagano, T.S., H. Aumann, S. Broberg, C. Canas, E. Manning, K. Overoye, R. Wilson, "SI-Traceability and Measurement Uncertainty of the Atmospheric Infrared Sounder Version 5 Level 1B Radiances", *Remote Sens.* 2020, 12, 1338; <https://doi.org/10.3390/rs12081338>
2. R. C. Coda, M. Tierney, "Radiometric Calibrator Thermal Analysis", LMIRIS DFN 94389, October 29, 1994
3. K. Overoye, "Measured BSDF and specular reflectance of Z302 paint used in AIRS OBC".

Introduction

The AIRS instrument On-Board Calibrator (OBC) blackbody provides a radiometric reference to the AIRS infrared channels in-orbit. Along with the space view, a two point calibration is obtained that is updated every scan line in the AIRS data products. The algorithm for radiometric calibration and the radiometric measurement uncertainty are described in detail in reference 1. Estimates of the emissivity and temperature of the OBC blackbody for AIRS were determined empirically by transfer from the Large Area Blackbody (LABB) during pre-flight calibration. Absolute measurements of these parameters has been estimated and used to determine the measurement uncertainty.

In this memo we provide two additional sources of information on the blackbody from the manufacture BAE Systems (Formerly Lockheed Martin Infrared Imaging Systems (LMIRIS)). 1. Measurements of the paint used in the OBC, Z302 manufactured by Aeroglaze (Appendix A), and 2. A thermal analysis of the OBC performed by LMIRIS (Appendix B).

Analysis

Appendix A shows the results from the Aeroglaze measurements. The specular reflectance of the paint is 10%-15% for steep angles (65°), and better than 7% at 25°. These measurements were used to determine the actual emissivity of the OBC with a result of 0.99988 (reference 1). Pre-flight measurements when compared to the LABB give an effective emissivity of 1.000 ± 0.002 . The pre-flight measurement is most likely limited by the ability to measure the OBC or viewing geometry differences between the OBC and LABB.

The temperature of the OBC was also determined by transfer of the calibration from the LABB. A nominal temperature of 308.2K was determined during this transfer. Since it is not possible to differentiate between a temperature difference or emissivity difference in the transfer of the calibration, no wavelength, or module dependence was applied to the OBC temperature. Any differences in the radiances observed between the OBC and LABB were removed using an 'effective' emissivity.

The LMIRIS thermal analysis (Appendix B) shows a 38 mK temperature gradient for the sloping surface, 130 mK for the vertical surface, and 316 mK for the triangular surfaces. The different AIRS modules (corresponding to different frequencies) image the pupil and could view different temperature gradients between the LABB and OBC. Figure 1 shows effective emissivity of the OBC used in Version 8 (left), and the temperature difference from the nominal 308.2K of the OBC needed to produce the same effect for a fixed emissivity (right).

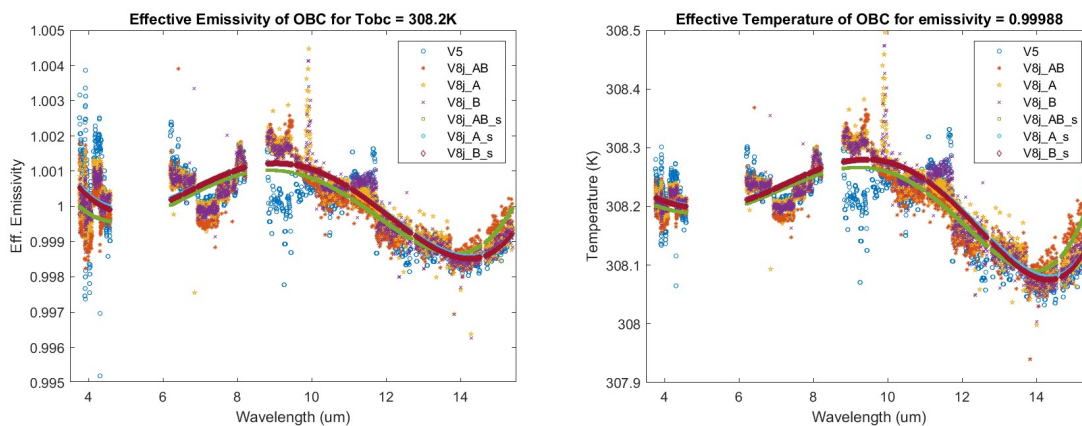


Figure 1 (Left), AIRS Effective Emissivity derived preflight from cross-calibration to the LABB, (Right) effective temperature that would produce an equivalent cross-calibration to the LABB.

Conclusions

In retrospect, using an 'effective' temperature of the OBC may have been more physical than an 'effective' emissivity, however, practically, both are equivalent, and both are empirically derived. Again, the data provided in the appendices have not been used directly in the calibration of the OBC, but have been used to estimate the measurement uncertainty in reference 1. It is provided here to enable researchers to better understand the instrument and explore alternative calibration approaches if desired. All calibration coefficients and data from the pre-flight radiometric response measurements viewing the LABB are provided on the AIRS website and the NASA GES/DISC.

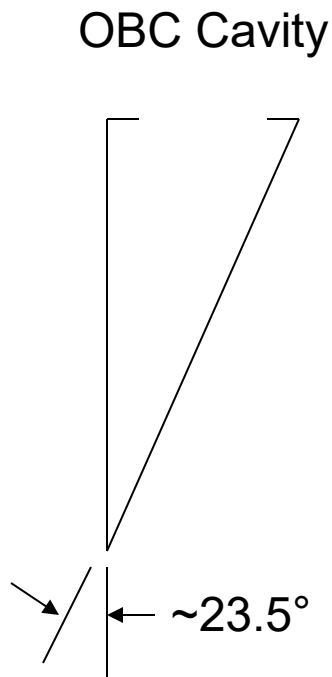
<https://airs.jpl.nasa.gov/mission/instrument-calibration/radiometric-ancillary/>

Acknowledgements

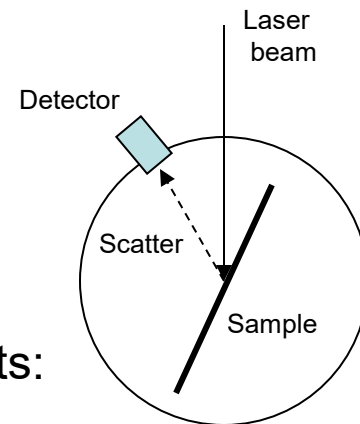
The research was carried out at the Jet Propulsion Laboratory, California Institute of Technology, under a contract with the National Aeronautics and Space Administration (80NM0018D0004). © 2025. California Institute of Technology. Government sponsorship acknowledged.

Measured BSDF and specular reflectance of Z302 paint used in AIRS OBC

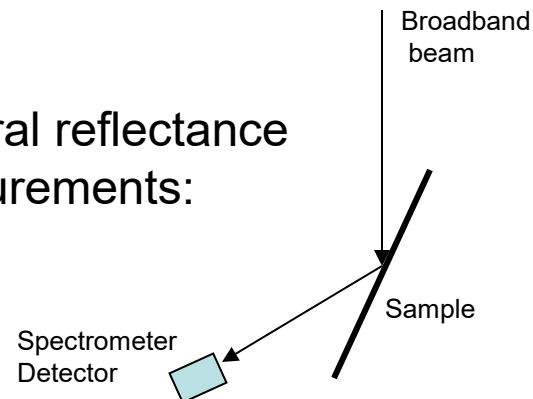
- Specular reflectance vs. wavelength measured in house on samples prepared in same manner as OBC interior surfaces
- BSDF of similarly prepared samples measured at TMA Technologies Inc, Bozeman, Montana.



BSDF measurements:

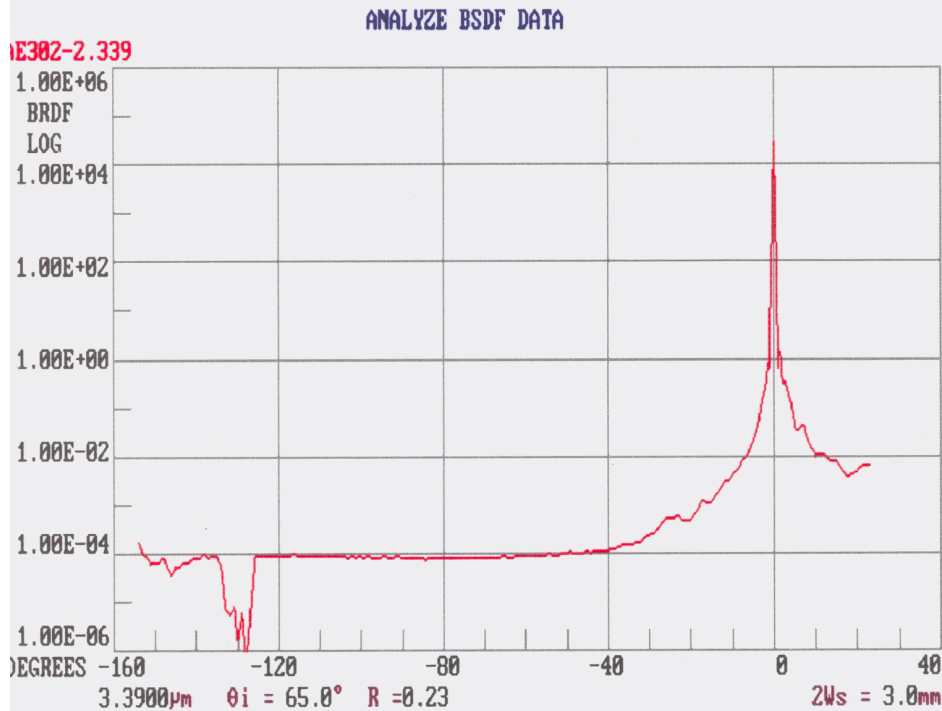


Spectral reflectance measurements:



Z302 BSDF @ 3.39 μm

Z302
BRDF @ 3.39 μm



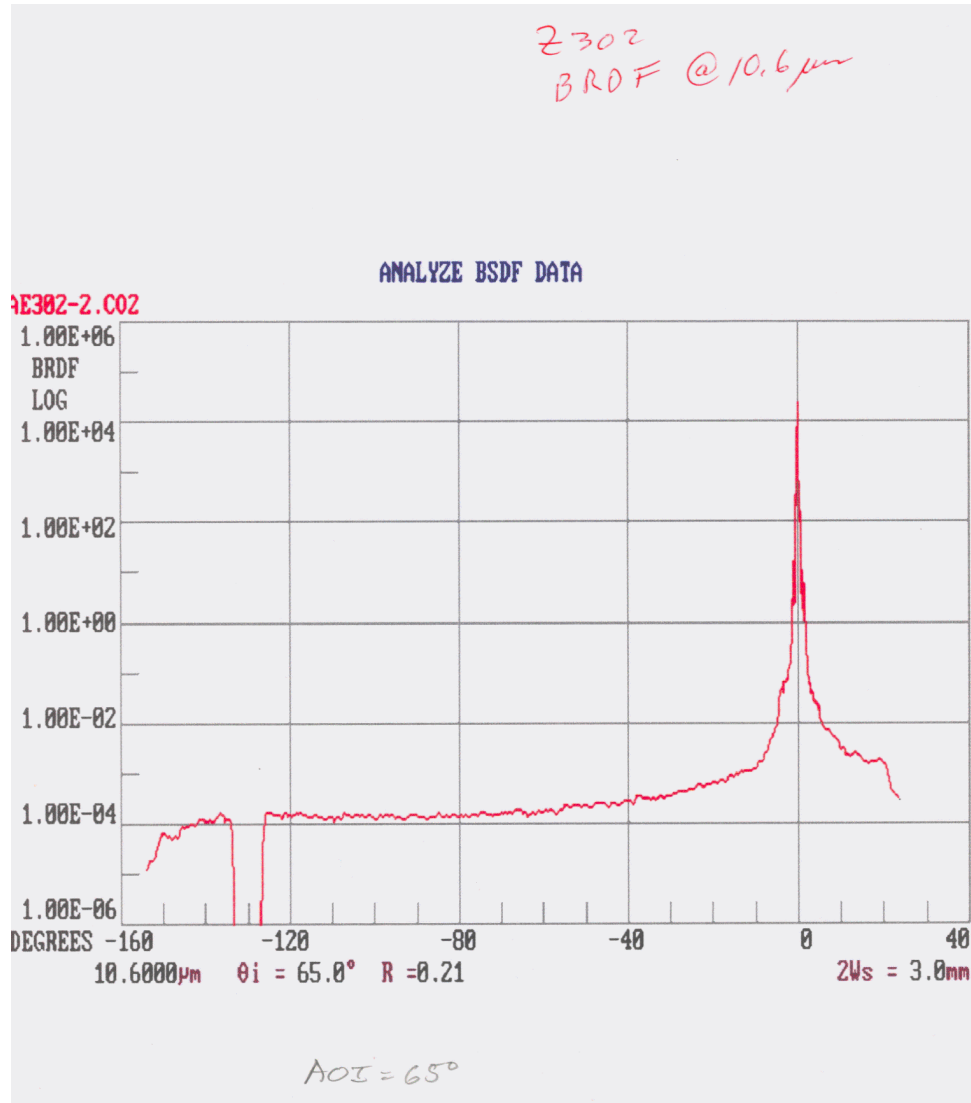
AOI = 65°

Angle of incidence on surface
= 65° (as in AIRS OBC)

Horizontal scale is angle in
degrees from the specularly
reflected direction; thus, back
scatter out of cavity is in the
direction $180 - 2 * 25^\circ = 130^\circ$.
That is the direction of the glitch
in the plot, where the detector
then interferes with the incident
beam.

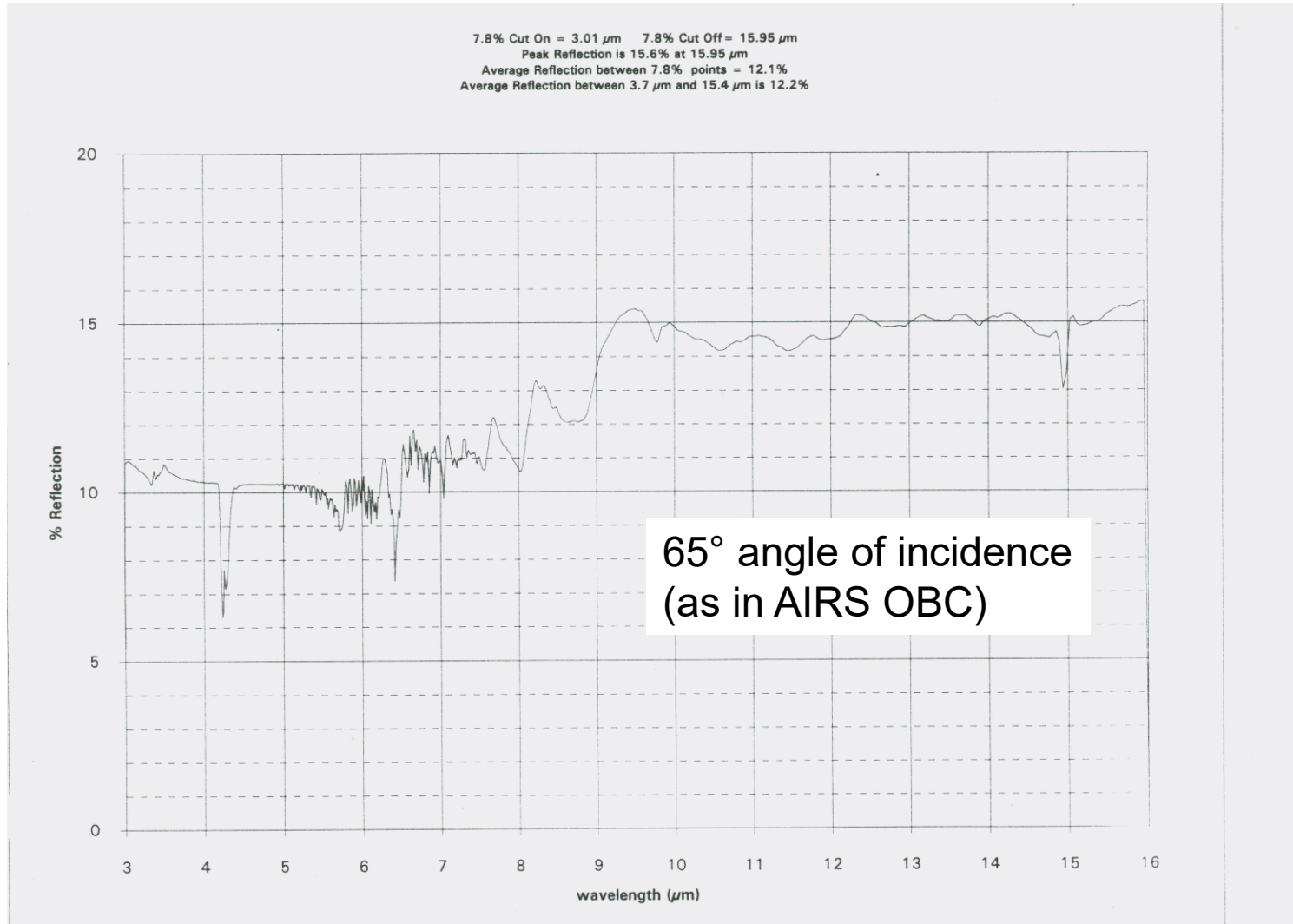
Vertical scale is BSDF in sr^{-1} .

Z302 BSDF @ 10.6 μm

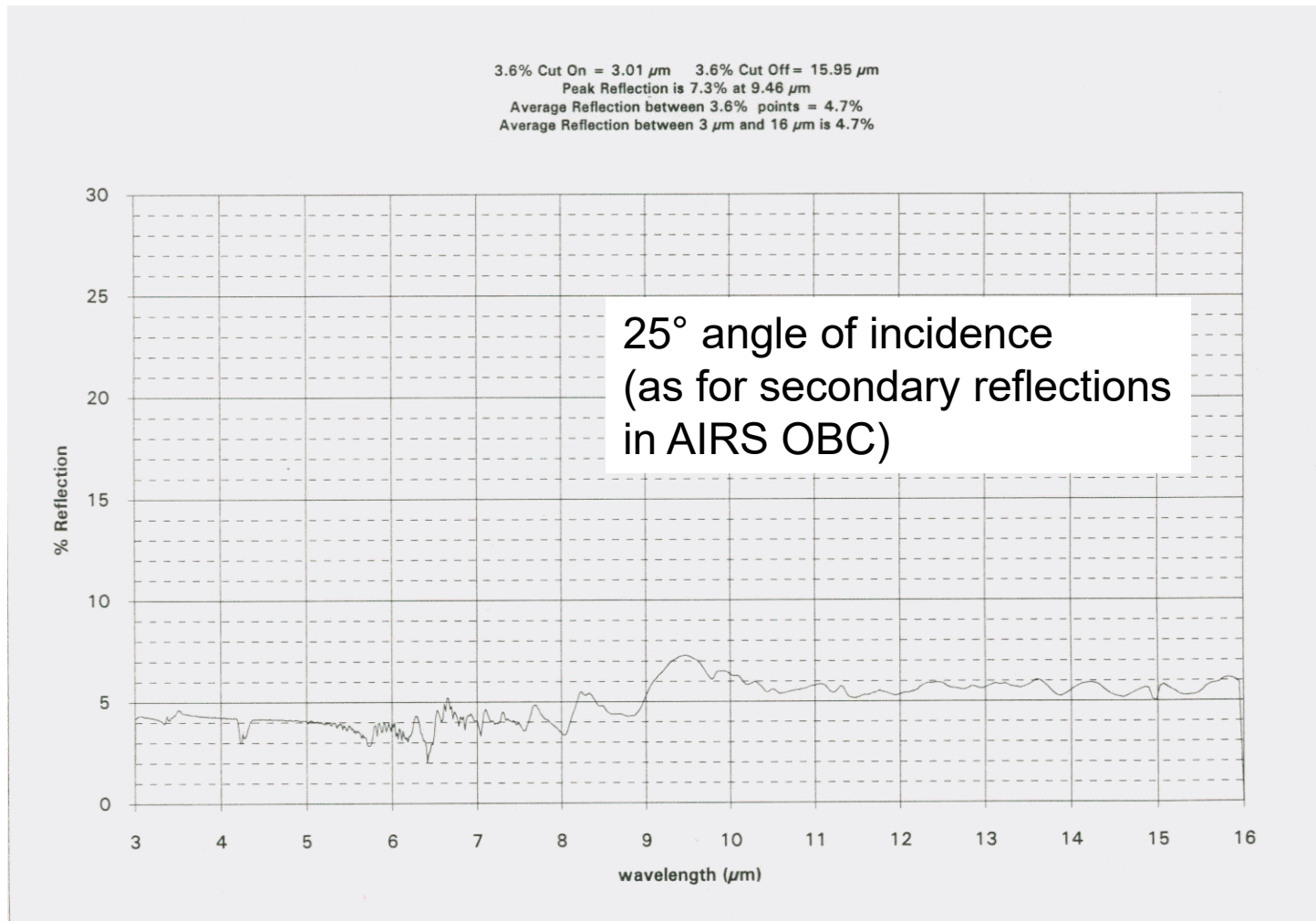


65° angle of incidence

Z302 Specular reflectance vs. λ



Z302 Specular reflectance vs. λ





DESIGN FILE COVER SHEET

| | |
|--|--|
| DATE OF DOCUMENT <div style="text-align: center; font-size: 1.2em;"> 29 OCT 94 DAY MONTH YEAR </div> | DESIGN FILE NUMBER <div style="text-align: center; font-size: 1.2em;"> 94389 </div> |
| AUTHOR(S) <i>R.C. COBA</i> <i>M. TIERNEY</i> | REFERENCE DOCUMENTS |
| TITLE <i>RADIOMETRIC Calibrator</i> <i>Thermal Analysis</i> | RESTRICTIONS <input type="checkbox"/> PROPRIETARY <input type="checkbox"/> COMPETITION SENSITIVE |

KEYWORD CHECKLIST

SELECT ONE SUBJECT AND ONE DOCUMENT TYPE

SUBJECT/SUBSYSTEM

DOCUMENT TYPE

- | | |
|--|---|
| <input type="checkbox"/> AIRS Calibration Facility <input type="checkbox"/> Aperture Cover <input type="checkbox"/> Bandpass Filters <input type="checkbox"/> Chopper <input type="checkbox"/> Configuration Management <input type="checkbox"/> Contamination Control <input type="checkbox"/> Electronics <input type="checkbox"/> Environments <input type="checkbox"/> Flight Software <input type="checkbox"/> FPA Cryosystem <input type="checkbox"/> Grating <input type="checkbox"/> Ground Support Equipment <input checked="" type="checkbox"/> In-Flight Calibration <input type="checkbox"/> Instrument Support <input type="checkbox"/> Integration & Test <input type="checkbox"/> IR Detector/Dewar <input type="checkbox"/> FPA ARCH. <input type="checkbox"/> PV <input type="checkbox"/> DEWAR <input type="checkbox"/> ROIC <input type="checkbox"/> PC <input type="checkbox"/> TEST | <input type="checkbox"/> IR Spectrometer <input type="checkbox"/> Mux Design <input type="checkbox"/> Mux Test <input type="checkbox"/> Parts, Materials, Processes <input type="checkbox"/> Photoconductive <input type="checkbox"/> Fab <input type="checkbox"/> Test <input type="checkbox"/> Photovoltaic <input type="checkbox"/> Design <input type="checkbox"/> Fab <input type="checkbox"/> Growth <input type="checkbox"/> Power Supply <input type="checkbox"/> Program <input type="checkbox"/> Quality Assurance <input type="checkbox"/> Radiative Cooler <input type="checkbox"/> Reliability/Maintainability/Safety <input type="checkbox"/> S/C Interface <input type="checkbox"/> Scanner <input type="checkbox"/> Systems Engineering <input type="checkbox"/> Thermal/Structural <input type="checkbox"/> Weight <input type="checkbox"/> VIS/NIR Sensor <input type="checkbox"/> Other |
|--|---|

- Analysis/Design Assumptions
- Design Documentation
- Specification
- General Memo
- Telecon
- Meeting Notes
- Customer Document
- Trip Report
- CDRL No. _____
- Technical Directive

- Possible New Technology Disclosure Required
- YES NO


DOCUMENT ENTERED INTO FILE SYSTEM

BY *CS* ON *11/2/94* (DATE)

DATE: October 29, 1994

SUBJECT: Radiometric Calibrator Thermal Analysis

TO: List


FROM: R.C. Coda
M.Tierney

ORGANIZATION: AIRS

LOCATION: Lexington

MS: 345

EXT: 4549

INTRODUCTION

The radiometric calibrator is one of three calibrators used for calibration in the AIRS instrument. Figure 1 shows the general configuration of the radiometric calibrator. The stringent thermal requirements placed on the blackbody cavity (herein referred to as cavity) for isothermalization require that the cavity be thermally isolated from its housing, be made of a high thermally conducting material and use a heater with controller to maintain it at the desired operating temperature. Thermally decoupling the cavity from its local environment achieves three purposes: (a) reduces heater power required to hold the cavity at the desired operating temperature, (b) reduces the local environmental temperature changes to acceptable levels and (c) reduces thermal gradients caused by heat flows away from the cavity. The thermal decoupling is achieved through the use of a low effective emittance coating on all the cavity's exterior surfaces and the housing interior, low conductance supports between the cavity and the housing and small wire size. The cavity's high internal conductivity helps to reduce its internal gradients to acceptable levels. The radiometric calibrator was analyzed to: (1) predict the thermal gradients for the on-orbit operational temperature extremes, i.e., the hot end-of-life (EOL) and the cold beginning-of-life (BOL) orbital conditions, (2) determine the temperature response to scan cycle and orbital influences and (3) define the locations for the temperature sensors and heaters. A thermal model of the radiometric calibrator was generated for use with the double precision SINDA/G thermal analyzer. The radiation coupling coefficients between the cavity and its aperture were determined with the TRASYS program. Steady state and transient conditions were considered.

REQUIREMENTS

The radiometric calibrator must meet the following three thermal requirements for the cavity during system operation: (1) operate at a temperature of 306-310K; (2) maintain

lateral temperature gradients within the "Zones of Interest" (refer to Figure 2) in each cavity surface as follows: $\leq 0.05\text{K}$ on the sloping surface, $\leq 0.15\text{K}$ on the vertical surface and $\leq 1.35\text{K}$ on the triangular surfaces and (3) maintain heater power to less than 2.5 Watts. In regards to requirement (2) above, the differences in lateral temperature gradient requirements between the cavity surfaces are best explained by noting that the contribution of photons emitted from a surface other than the sloping surface is related to the number of bounces to get to the sloping surface and then into the spectrometer's field of view. The contribution from each surface other than the sloping surface is 3^n (input from Systems group) where n is the least number of bounces a photon must take upon leaving a surface to get to the sloping surface and then leaving the cavity. Since the vertical surface must make a minimum of one bounce and the triangular surfaces must make a minimum of 3 bounces (input from Systems group) before leaving the cavity, their temperature gradients were ratioed by the application of the above surface contribution formula to be: $3^1 * 0.05\text{K} = 0.15\text{K}$ for the vertical surface and $3^3 * 0.05\text{K} = 1.35\text{K}$ for the triangular surfaces.

THERMAL MODEL DESCRIPTION

Prior to the development of a detail thermal model of the radiometric calibrator's cavity, initial calculations were performed which defined the thermal control concept. These calculations established the coatings, the amount of conductive and radiative isolation and the heater power. To verify that the design concept could meet the small temperature gradient requirement for the sloping surface a detail thermal model of the cavity was generated. This model could then confirm the initial calculations.

The detail thermal model of the radiometric calibrator consisted of 425 nodes: 50 nodes on each of the four sides of the cavity, 18 nodes for aperture edge, 200 nodes representing the paint surface (each paint node corresponded to a cavity node), 5 nodes for the aluminum housing and 2 additional nodes representing boundary conditions (Figure 2).

The following lists the thermal properties of the various radiometric calibrator materials used in the analysis.

| Property/Material | Al 1100 | Beryllium | Titanium | Black Paint Z302 |
|-------------------------------|---------|-----------|----------|------------------|
| Thermal Conductivity (W/cm-K) | 2.20 | 1.72 | 0.086 | 0.002 |
| Specific Heat (J/g-K) | 0.93 | 1.88 | 0.65 | 1.50 |
| Density (g/cm ³) | 2.71 | 1.85 | 1.36 | 1.2 |
| External Surface Emissivity | 0.05 | 0.05 | 0.05 | 0.912 |

The temperature gradient in the sloping surface is dependent upon the radiant view factor between the walls and the aperture. Since this view factor changes with position along the sloping surface, it was necessary to generate a TRASYS model of the cavity surfaces. This resulted in generating approximately 2500 radiation conductors representing the radiant interchange between the cavity nodes and between the cavity nodes and the aperture. Properties used for the black paint are listed in the above table.

Heat losses between the cavity and its housing must be held to a minimum to reduce power levels required for thermal control and to meet the gradient requirements. This is achieved by conductively and radiatively isolating the cavity from the housing. Conductive isolation was achieved initially with six stainless steel supports. The combined area to length ratio (A/L) for these supports was 0.0469 inches. The support surfaces were coated with vapor deposited gold to reduce their radiative coupling with the environment. Radiative isolation of the cavity is achieved using a low emissivity coating (vapor deposited gold) with an effective emittance of 0.05 or less. This coating is required on the exterior of the cavity and the interior of the housing. To reduce the thermal influences of the local environment surrounding the housing, a low emittance coating on the housing's exterior surface is required. The model assumes that MLI (effective emittance ≤ 0.02) will be placed over all calibrator housing exterior surfaces to reduce radiation coupling to the surrounding environment.

In the model the wires which connect the heater and temperature sensors consisted of 32 wires of 30 gauge copper.

Three versions of the detail thermal model were constructed to evaluate the effects of environmental boundary conditions. A steady state version and two transient versions. The two transient versions consisted of an orbital transient model and a scan cycle transient model. For the orbital transient and steady state simulations the rotating baffle's scan cycle thermal influence is small and therefore an effective emissivity for the rotating baffle was calculated. The value used was 0.1. This value represents the rotational average emittance over a single scan cycle.

1. STEADY STATE MODEL and MODEL EVOLUTION

The steady state model did assess the impact of the BOL and EOL boundary conditions on the gradient. However, a large part of the steady state runs considered the cold boundary conditions, since these conditions produced the largest gradients in each of the cavity's surfaces.

The initial part of the thermal analysis utilized the steady state model to iteratively evaluate the influence on each surface's gradient due to: (1) the impact of heater location, its power dissipation, and its size, (2) the support locations, number of supports, and support thermal isolation, (3) the cavity wall thickness and (4) wire heat sink location. Many cases were run to arrive at the heater location, size and power dissipation to achieve the requirements of power dissipation and temperature gradient

on each surface. Initial studies began with 1100 series aluminum. 1100 aluminum was chosen because of its high thermal conductivity. However, due to weight constraints, the cavity material was changed to beryllium which has a thermal conductivity close to 1100 aluminum (refer to the Property table above).

Initial trial cases run with the thermal model indicated that the wire bundle which was originally heat sunk to the vertical surface produced an unacceptable localized temperature depression in this surface. Since the thermal influences of the triangular surfaces are less dominant, it was decided to split the wire bundle in two bundles (one half of the wires in each bundle) and heat sink each of these smaller bundles in the center of each triangular surface.

Local temperature depressions in the vertical and triangular sides produced by three of the six supports became an undesirable feature. Refined structural analysis indicated that the number of supports can be reduced from six to three and that the material could change from stainless steel to titanium. These changes achieved a higher degree of conductive isolation and removed the local temperature depressions in the vertical and triangular sides. With this change to the supports the new combined (A/L) is 0.0346 inches.

During the initial steady state runs the paint coating was not considered separately as separate nodes. However, as the analysis became more refined, it became necessary to incorporate the paint as separate nodes. Now the model has a corresponding paint node for each cavity node for a total of 200 paint nodes. The paint thickness was taken to be 0.005 inches and the paint properties are in the above table.

2. TRANSIENT MODELS

Two versions of the transient model were generated: one to assess the orbital environmental boundary conditions (orbital transient model) and one to evaluate the scan cycle perturbations (scan cycle transient model).

The orbital transient model determined the dynamic effects of the changing orbital environment on the cavity. Heater power was applied (at a constant setting) to maintain the desired operating temperature, but no control of this temperature was made. The AIRS instrument system thermal model was exercised to determine the orbital temperature of the scan housing (Figure 3) which served as a boundary condition for the radiometric calibrator in orbital transient model.

In the scan cycle transient model the rotating baffle also acts as a time varying boundary condition which influences the paint surface temperature. The baffle which is viewed directly by the internal surfaces of the cavity rotates once every 2.667 seconds. During this rotation period, the opening in the baffle is viewed by the cavity for 22.5 milliseconds (ms) and appears for most of this time period as a blackbody at 273K in a hot case condition and 263K during a cold case condition. For 3 ms period within the

RESULTS

Although all six cases were evaluated, only the last three are presented herein. Results showed that these three cases ("cold case" conditions) produced the largest thermal gradients within the cavity.

Case 4 results indicate the sensitivity of the cavity to the rotating baffle temperature and emissivity changes. Results indicate that the center portion of the cavity's sloping surface shows a peak to peak thermal response of 0.018K on the black paint's surface due to the rotating baffle effects (see Figures 5 and 6). This small temperature change is a result of the relatively short period during the cycle (22.5ms) that the cavity views the rotating baffle opening. These results indicate that the thermal gradient stability affects of the rotating baffle on the beryllium substrate are negligible but the paint surface temperature change is larger. Discussions with the Systems group indicate that this thermal response in the paint's surface is acceptable since its knowledge is known and is within the allowed budget of 0.03K.

Case 5 results show the affects of orbital temperature variations on the cavity's thermal gradient stability. Figures 7 shows the temperature variations of each surface of the cavity as a function of time during a single orbital period. These results indicate that the thermal stability of the sloping surface is $\pm 0.0193\text{K}$. Since the orbital temperature changes occur over a relatively long period compared to the scan period (2.67 seconds vs 98.8 minutes) and since knowledge of the cavity's temperature prior to each scan cycle is known, a temperature stability requirement for orbital temperature change is not required.

Case 6 determined the magnitude of the lateral temperature gradients produced on the cavity's surfaces as a result of the imposed boundary conditions. For the present configuration, the worst case lateral gradients for the "Zones of Interest" of each surface (refer to Figure 2) were found to be as follows: 0.038K on the sloping surface, 0.130K on the vertical surface, 0.316K for each triangular surfaces. Gradient results for all surfaces meet their requirements. Shown in Figure 8 is a contour temperature plot for the four internal surfaces indicating where these lateral gradients exist.

During normal operation the cavity's temperature is controlled to 306-310K with a foil heater, temperature sensors and controller. The heater is bonded to the sloping surface's exterior at the outside edges and extends from the bottom edge (at aperture) up to 80% of its full length (Figure 1). Additional results from this analysis indicate that the heater power required to maintain the radiometric calibrator at it's nominal operating temperature of 308.5 K varies between 0.182 watts for the hot case EOL conditions to 1.76 watts for the cold case BOL conditions.

CONCLUSIONS

The initial analyses on the radiometric calibrator were done assuming that the cavity was constructed of 1100 series aluminum. Although the results of those analyses showed a decrease in the temperature gradients within the cavity constructed of aluminum, beryllium was selected as the cavity material because of the savings in weight.

To find the heater location and power distribution which could satisfy the temperature gradient requirements for the sloping side, numerous steady state runs using the cold boundary conditions were made. As a result of those studies, the location proved to be along the outer edges of the sloping surface but terminating 1.65 inches short of the intersection of the sloping and vertical surfaces. This makes the physical size of the heaters 0.85 x 6.62 inches each. Although this design does require two separate heaters, they should be wired in series with a single controller.

The steady state analyses indicate that the thermal gradient requirements can be met for the "Zone of Interest" on all surfaces. The orbital analyses indicate that the expected orbital temperature variations for the cavity are acceptable. However, a temperature controllability requirement is required for the electronics circuit design but this requirement has not been defined at this time. Further analyses (thermal and systems) are required to determine what this requirement would be.

TEMPERATURE SENSORS

Temperature sensor locations are indicated in Figure 9. The locations presented here represent the minimum number and are a result of discussions and agreement with the Systems Group. The location, temperature range, initial accuracy and stability over life requirements for these sensors are indicated below:

| Location | Temperature Range (K) | Initial Accuracy (K) | Stability over life (K) |
|----------|--|----------------------|-------------------------|
| T1 | Control: 306 to 310 270 to 306 & 310 to 330 | 0.02 1.0 | 0.02 - |
| T2 | 306 to 310 270 to 306 & 310 to 330 | 0.02 1.0 | 0.02 - |
| T3 | 306 to 310 270 to 306 & 310 to 330 | 0.02 1.0 | 0.02 - |
| T4 | 306 to 310 270 to 306 & 310 to 330 | 0.02 1.0 | 0.02 - |

Temperature sensor location T1 has been selected as the control point for the heater control circuit.

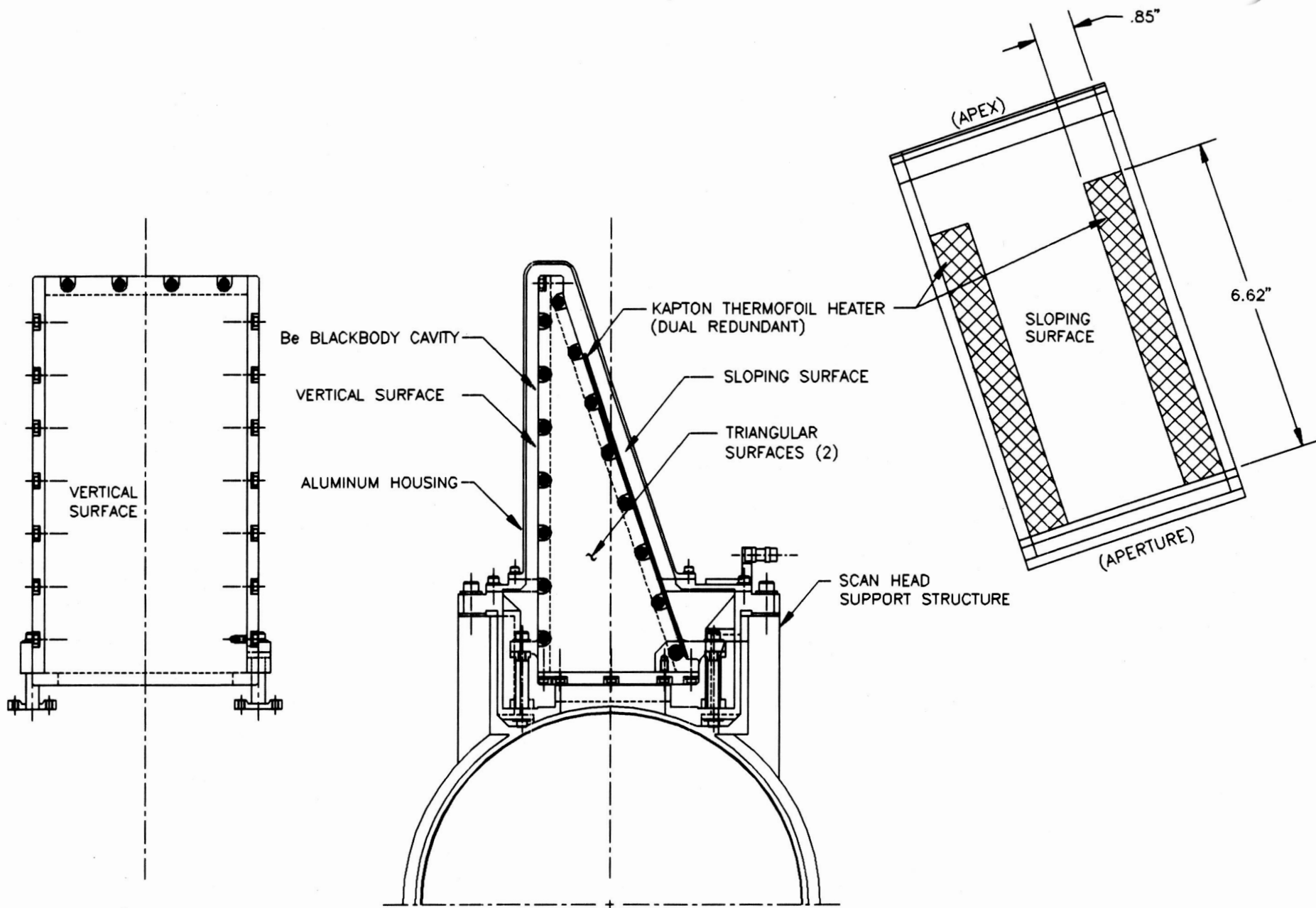


FIGURE 1
 RADIOMETRIC CALIBRATOR ASSEMBLY

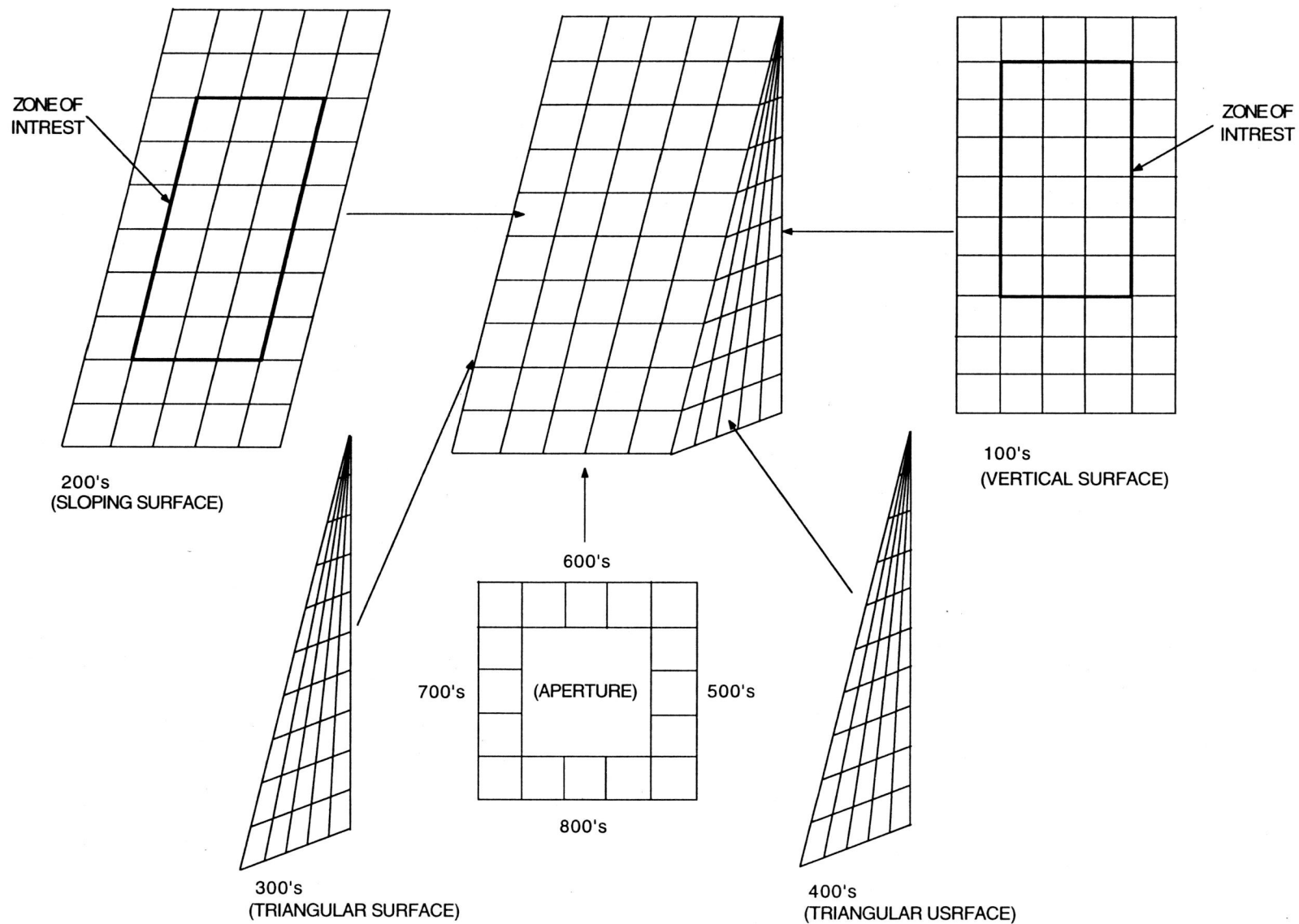
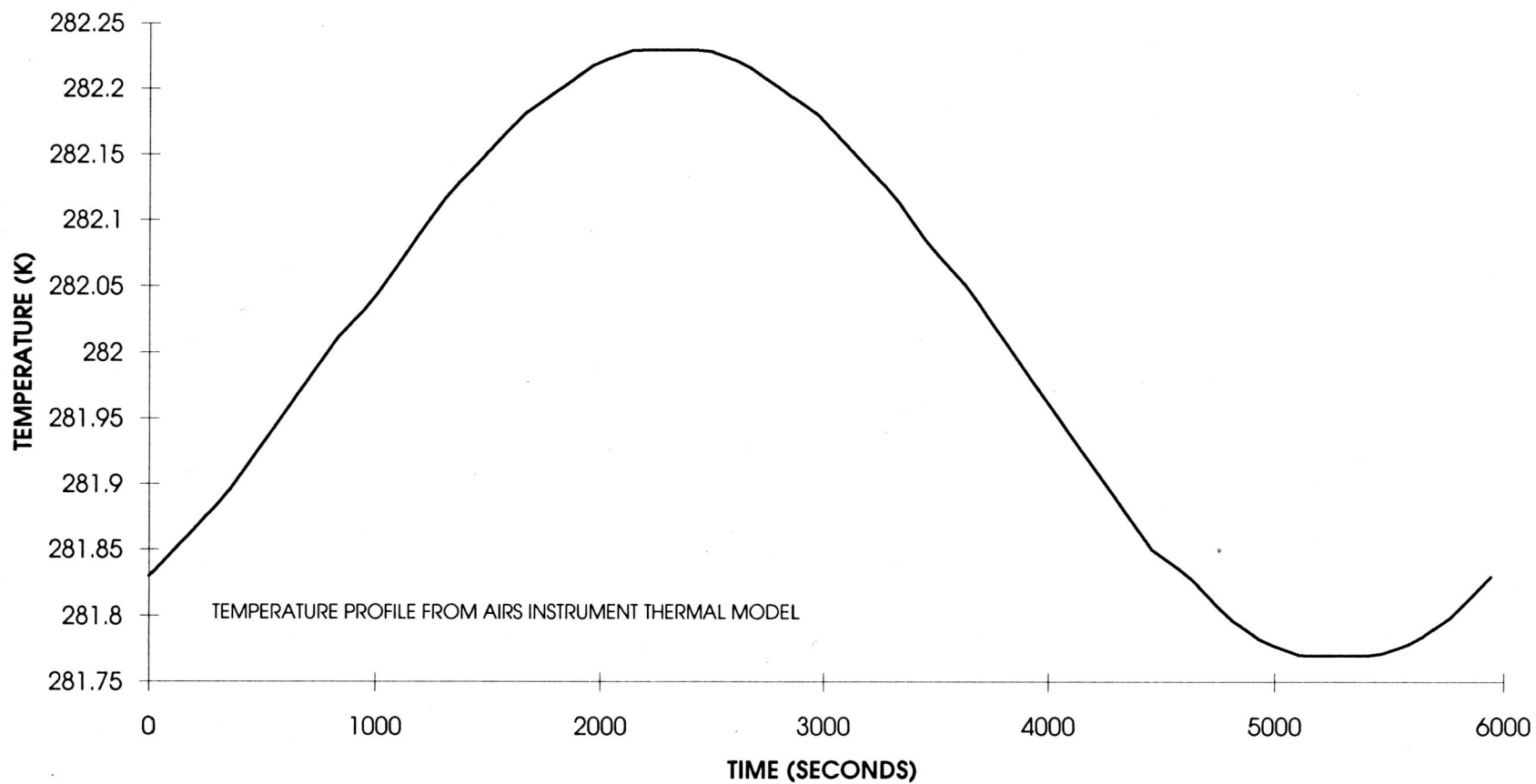


FIGURE 2
 RADIOMETRIC CALIBRATOR THERMAL MODEL

FIGURE 3
SCAN HOUSING TEMPERATURE PROFILE



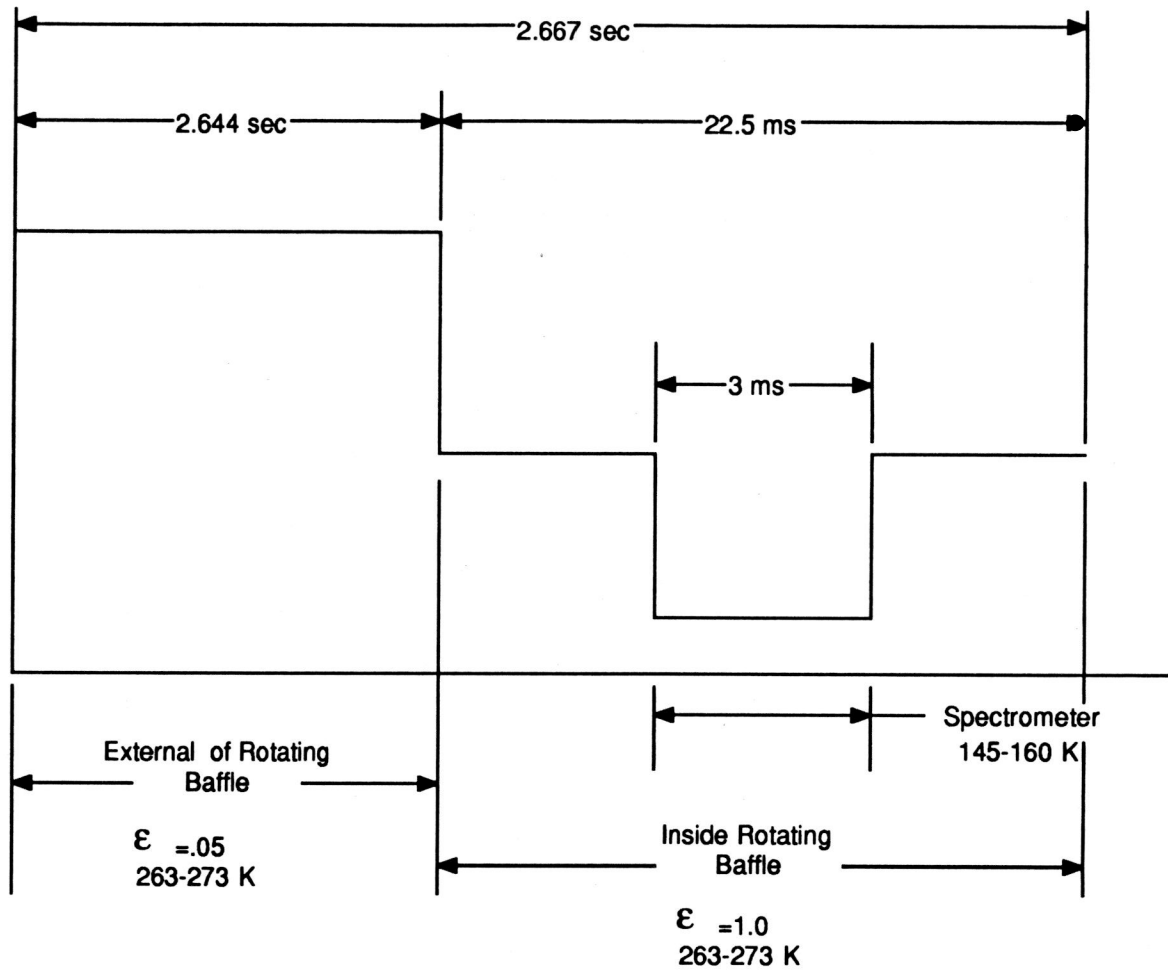


FIGURE 4
BOUNDARY CONDITION OF ROTATING BAFFLE

FIGURE 5
RADIOMETRIC CALIBRATOR THERMAL RESPONSE TO SCAN CYCLE

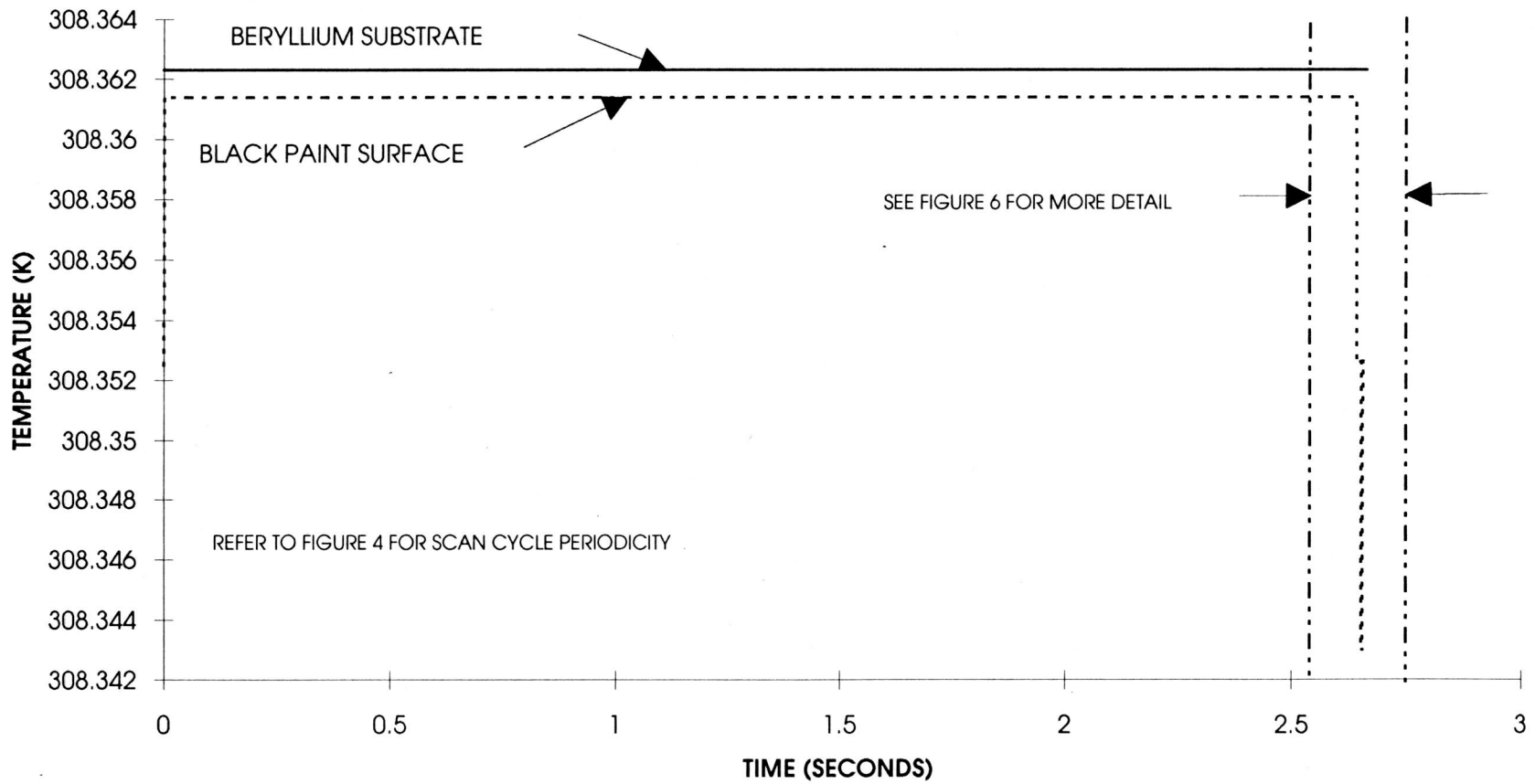


FIGURE 6

RADIOMETRIC CALIBRATOR THERMAL RESPONSE DURING SPECTROMETER VIEWING

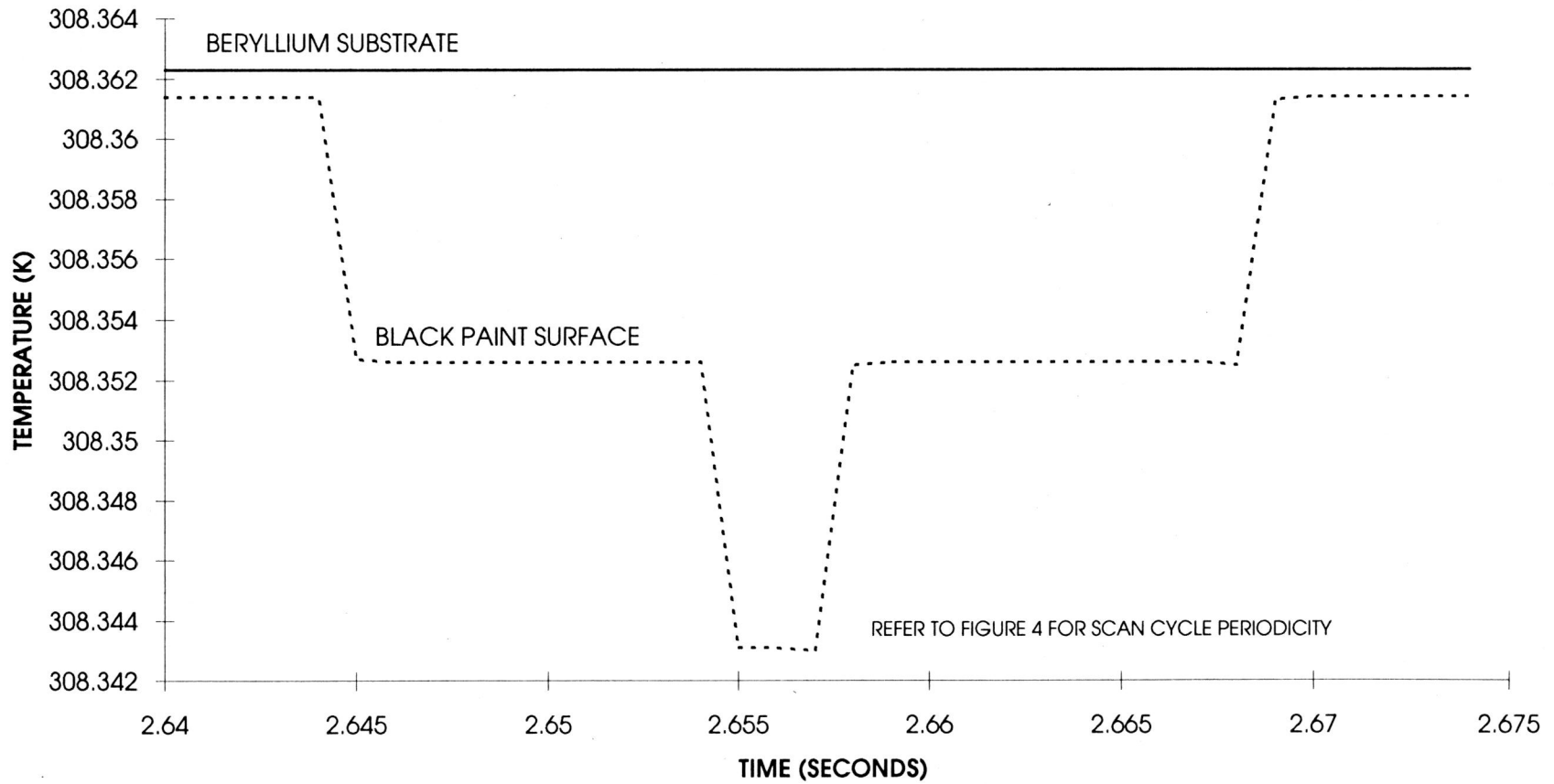
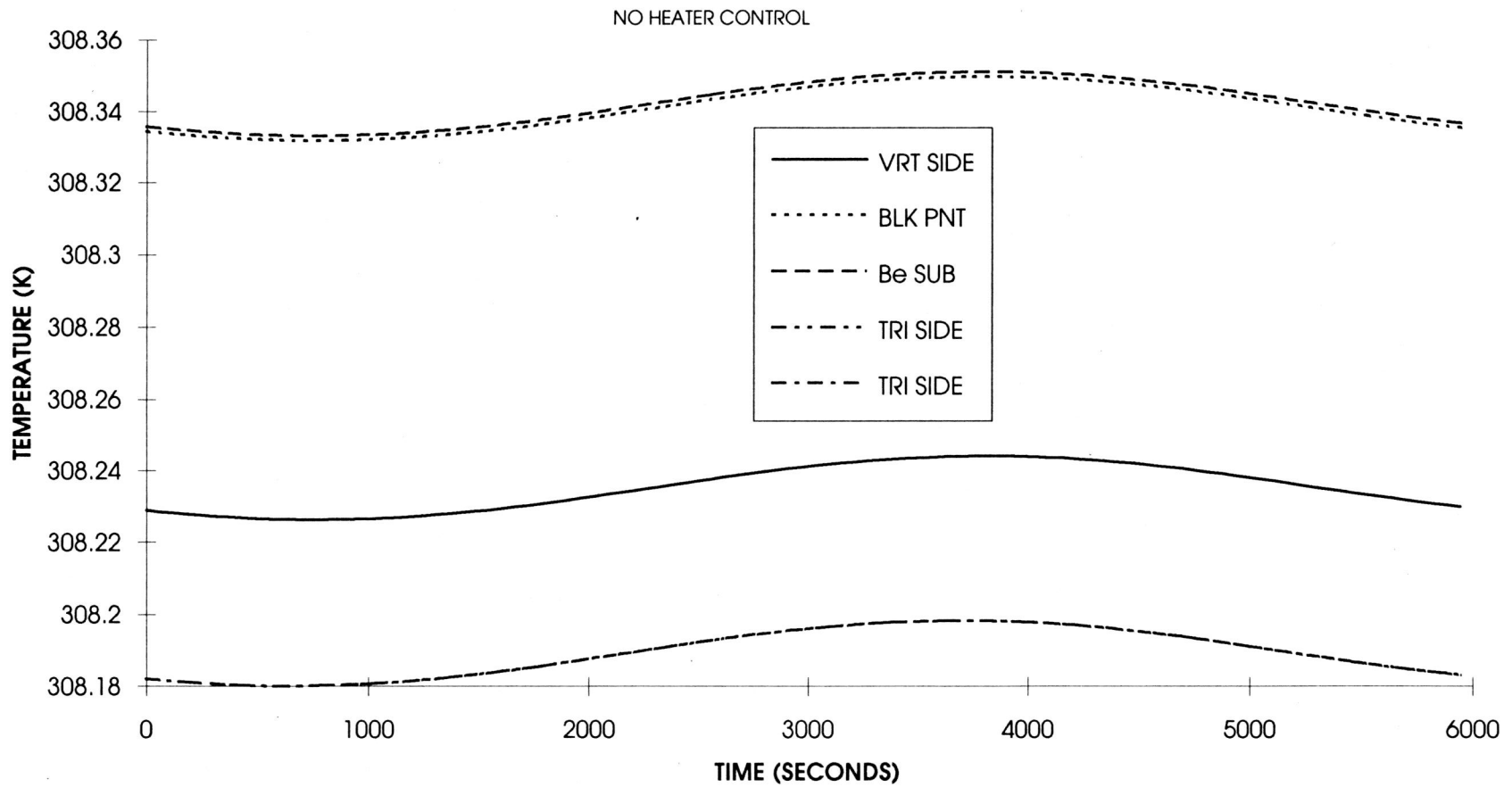


FIGURE 7
BLACKBODY CAVITY ORBITAL TEMPERATURE PROFILE



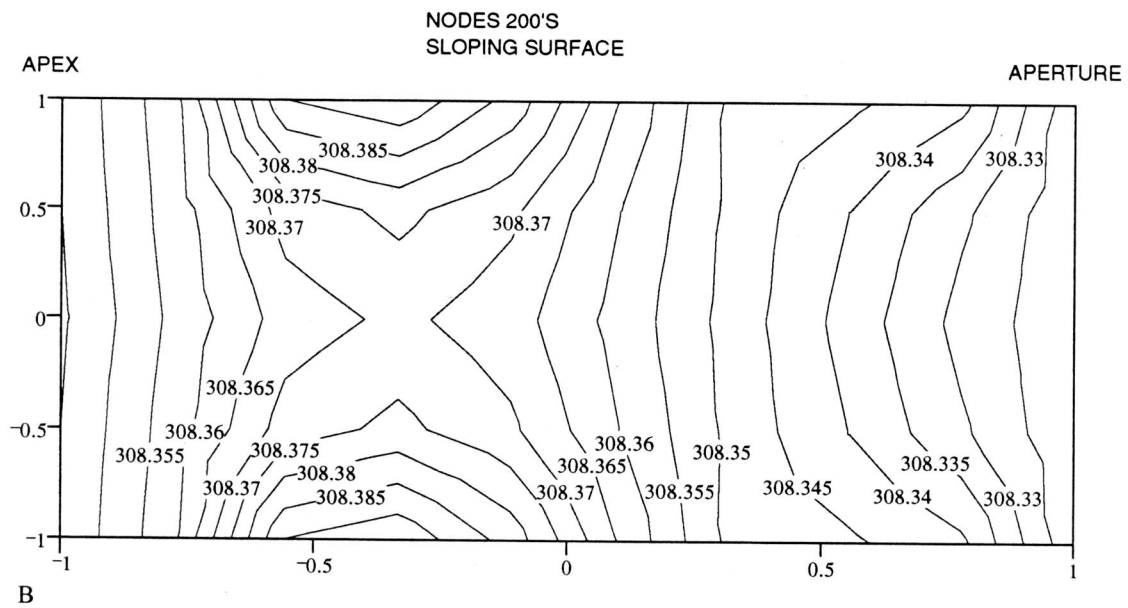
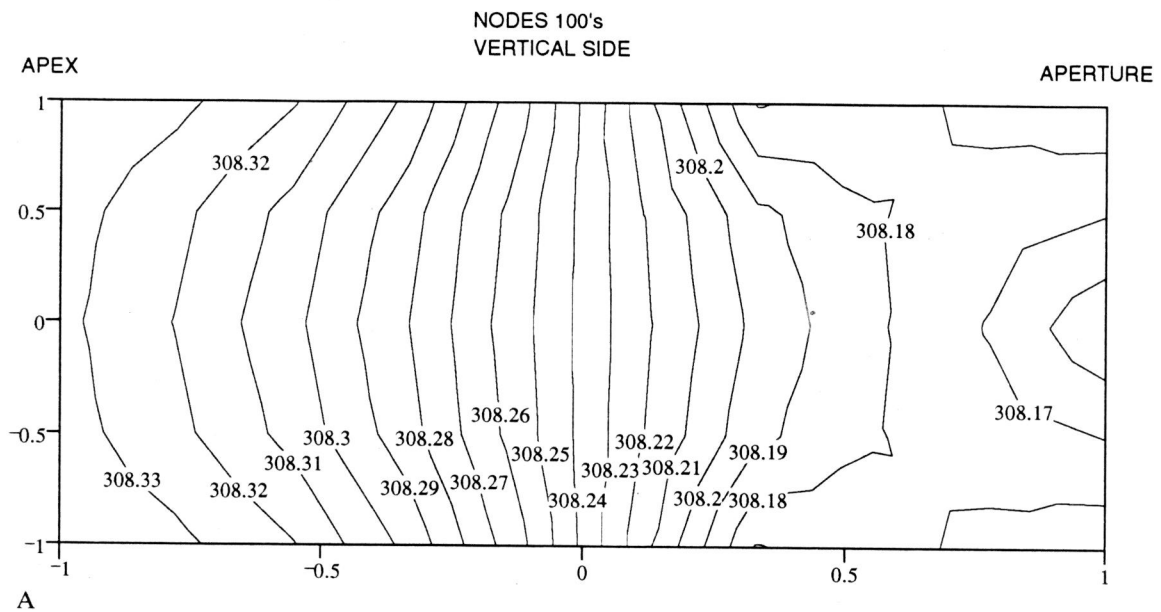


Figure 8 Blackbody Cavity Contour Temperature Plot in Degrees K

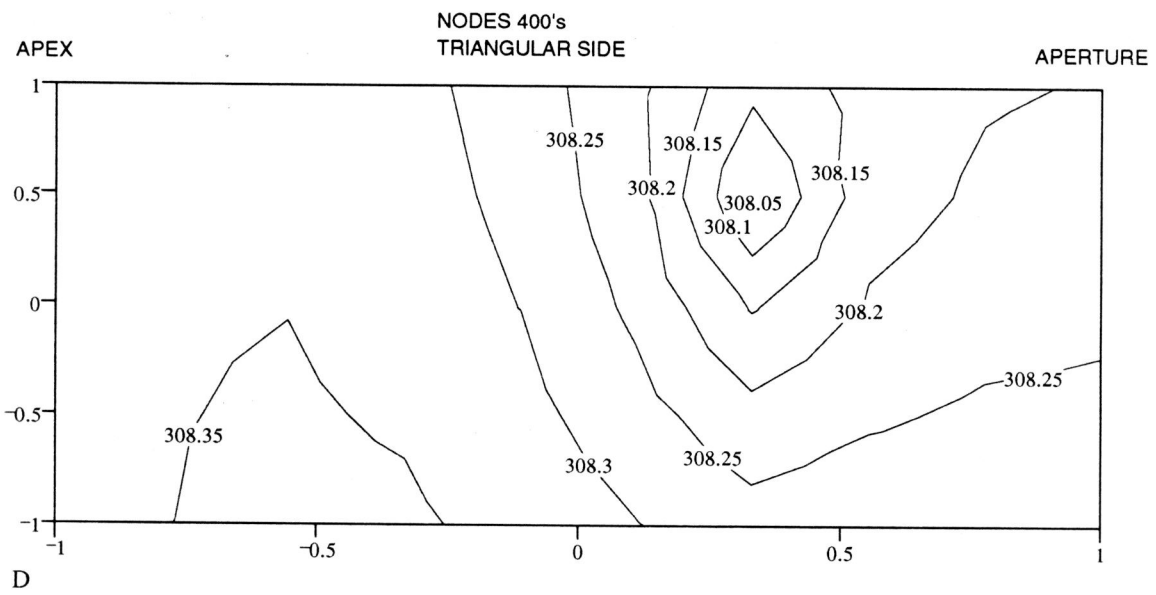
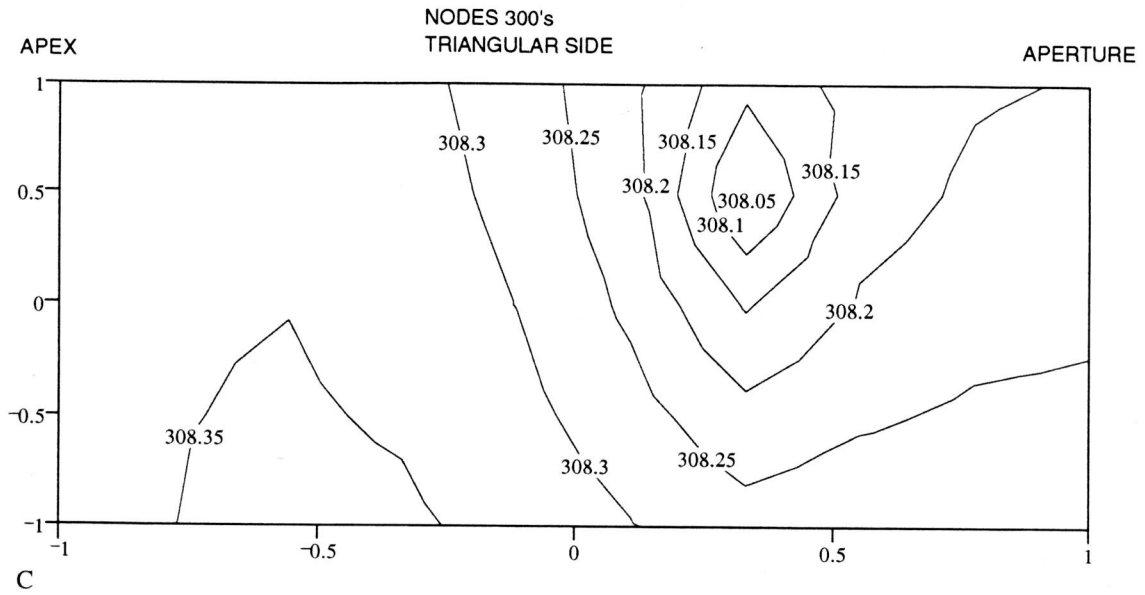


Figure 8 (cont) Blackbody Cavity Contour Temperature Plot in Degrees K

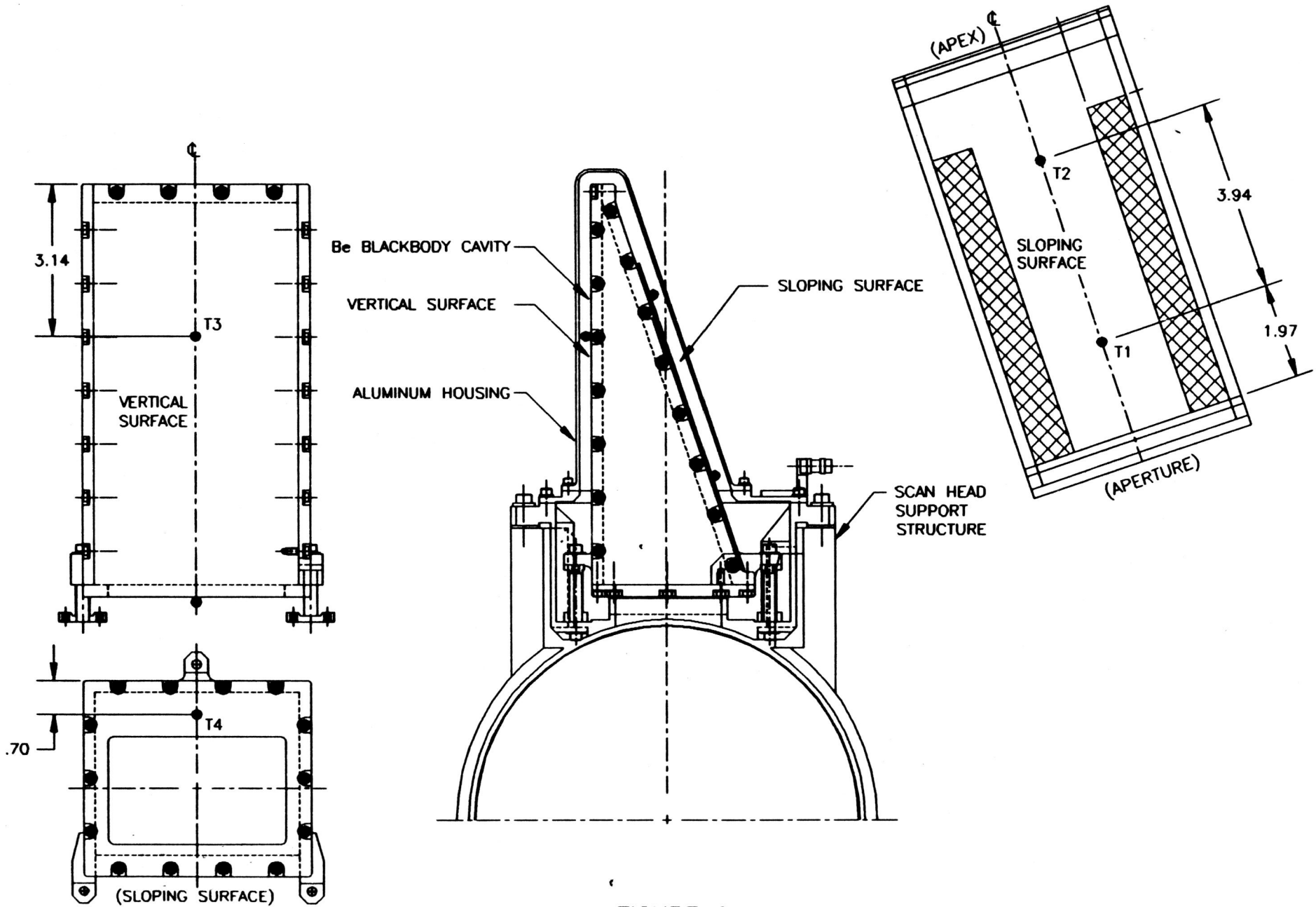


FIGURE 9
 TEMPERATURE SENSOR LOCATIONS

AIRS DISTRIBUTION LIST

| EMPLOYEE NAME | EXT. | M/S | ACTION | INFO |
|-------------------------|------|-----|--------|------|
| Aldrich, Nancy | 3198 | 285 | | |
| Azhand, Monagher | 4865 | 188 | | |
| Bates, Jerry | 3594 | 209 | | |
| Beaulieu, Paul | 4185 | 130 | | |
| Birkholz, Lori | 3090 | 146 | | |
| Boisvert, Nancy | 3052 | 209 | | |
| Callahan, Jack | 3445 | 243 | | |
| Campoli, Peter | 4320 | 242 | | |
| Carbone, Anthony | 4479 | 209 | | |
| Carita, Anthony | 3046 | 209 | | |
| Casey, Jim | 3291 | 242 | | |
| Coda, Roger | 4549 | 345 | | X |
| Colarusso Jr, Frederick | 3340 | 285 | | X |
| Cruikshank, Susan | 3103 | 130 | | |
| Dehne, John | 3300 | 105 | | |
| Dehorsey, Thurlow | 4692 | 242 | | |
| Desimone, Henry | 4823 | 244 | | |
| Dustin, Paul | 3150 | 209 | | |
| Evans, Lori | 3799 | 355 | | |
| Faria, Fernando | 4822 | 285 | | X |
| Fenske, David | 3104 | 209 | | |
| Fialli, Mark | 5224 | 342 | | |
| Flint, Neal | 3548 | 391 | | |
| Frost, Edmund | 3773 | 391 | | |
| Garnett, James | 4378 | 188 | | |
| Green, Kenneth | 3528 | 345 | | X |
| Groom, Dianne | 3843 | 209 | | |
| Gurnee, Mark | 3077 | 146 | | |
| Hanna, Joceline | 4171 | 112 | | |
| Hartle, Nancy | 3061 | 146 | | |
| Hassler, Richard | 4168 | 345 | | |
| Hatch, Marcus | 3533 | 345 | | |
| Hutton Jr, Thomas | 3764 | 121 | | |
| Hyde, Brian | 3051 | 386 | | |
| Jaworski, Frank | 3933 | 188 | | |
| Jayakumar, Marathurai | 4570 | 242 | | X |
| Jungkman, David | 3093 | 146 | | |
| Kachmarsky, James | 3212 | 345 | | X |
| Kacir, Thomas | 3808 | 242 | | |
| Kimball, Paulette | 3074 | 188 | | |
| Kleinmann, Douglas | 3841 | 117 | | |
| Krueger, Eric | 3659 | 146 | | |
| Krueger, Martha | 3105 | 146 | | |
| Lancaster, Robert | 3040 | 110 | | |
| Littlehale, Bob | 3629 | 242 | | |
| Marciniec, John | 4174 | 146 | | |
| Maschhoff, Kevin | 3900 | 146 | | |
| McHugh, David | 4348 | 209 | | |
| McKay, Thomas | 4067 | 345 | | |

| EMPLOYEE NAME | EXT. | M/S | ACTION | INFO |
|----------------------|------|-----|--------|------|
| Miller, Christopher | 3344 | 285 | | X |
| Morse, Paul | 3349 | 285 | | X |
| Norton, Peter | 3096 | 146 | | |
| O'Sullivan, Paul | 3546 | 285 | | X |
| Overoye, Ken | 3762 | 285 | | X |
| Pollock, Randy | 3574 | 285 | | X |
| Quann, David | 3229 | 146 | | |
| Reine, Marion | 3043 | 146 | | |
| Ricci, Louis | 4579 | 242 | | |
| Riddle, Kenneth | 3373 | 142 | | |
| Rigby, Paula | 3648 | 393 | | |
| Roderick, James | 4610 | 345 | | |
| Rutter Jr, James | 3078 | 146 | | |
| Sanford, Ron | 3967 | 285 | | |
| Shaw, Will | 3404 | 285 | | |
| Siegel, Andrew | 4230 | 188 | | |
| Southern, Arlene | 4501 | 340 | | |
| Staley, Wayne | 3948 | 345 | | |
| Stobie, James | 3075 | 188 | | |
| Thurgood, Alan (USU) | | | | |
| Tsao, Ray | 3709 | 285 | | |
| Vazquez, Carmelo | 4563 | 393 | | |
| Verrilli, Anthony | 3133 | 146 | | |
| Wagner, Kenneth | 3545 | 340 | | |
| Weiler, Margaret | 3825 | 146 | | |
| Wellman, Roxanne | 4310 | 117 | | |
| Willis, Nancy | 3294 | 209 | | |
| Wittels, Jill | 4821 | 141 | | |
| Wolfe, Tom | 4478 | 345 | | |
| Zimmermann, Peter | 3106 | 146 | | |
| Design File | 4501 | 340 | | X |
| HU, STEVE | | | | X |
| TIERNEY, MIKE | | | | X |